TALTECH
GEOLOOGIA INSTITUUT

Composition and geotechnical properties of paleo-weathering crust from the Vihterpalu F332 drill core

Bachelor thesis

Student: Carina Potagin (164338YAEB)

Supervisor: Rutt Hints, Researcher, PhD

Study programme: Earth Sciences and Geotechnology (YAEB)

Tallinn 2021

Autorideklaratsioon

Kinnitan, et olen koostanud antud lõputöö iseseisvalt ning seda ei ole kellegi teise poolt varem kaitsmisele esitatud. Kõik töö koostamisel kasutatud teiste autorite tööd, olulised seisukohad, kirjandusallikatest ja mujalt pärinevad andmed on töös viidatud.

Autor: Carina Potagin

[allkiri ja kuupäev]

Töö vastab bakalaureusetööle/magistritööle esitatavatele nõuetele.

Juhendaja: Rutt Hints

[allkiri ja kuupäev]

Töö on lubatud kaitsmisele.

Kaitsmiskomisjoni esimees: Olle Hints

[allkiri ja kuupäev]

Contents

Abstract

The thesis addresses geochemical and geotechnical properties of the Neoproterozoic paleo-weathering crust of the Estonian crystalline basement from the Vihterpalu F332 drill core. Interest towards a better characterization of such complexes has lately increased due to several perspective deep-infrastructure projects. The paleo-weathering crust of the crystalline basement in the Vihterpalu area lies in approximately depth 200 m and is covered by Phanerozoic sedimentary rocks. The paleo-weathering crust there has evolved on Si-poor magnetite-rich amphibolites.

For the study, 23 samples were collected from the paleo-weathering profile. All samples were analysed using X-ray diffraction and X-ray fluorescence techniques to characterize chemical and mineralogical variations in the weathering profile. Additionally, eight selected samples were used for geotechnical tests to determine parameters such as point load index, grain density, porosity, and also for microscopic studies.

Based on the results, the weathering crust was divided into three sections: paleosol (1.0 m), saprolite (4.0 m), and saprock (29.0 m). The uppermost red clay-rich paleosol horizon is highly weathered residual complex with CIW and CIA index > 90. Its mineral assemblage is composed of kaolinite, hematite, illite-smectite, and illite. Greenish saprolite horizon with secondary mineral complexes and signs of pervasive geochemical alteration showed complex Fe-Mg-rich clay mineral assemblage with celadonite. The study is the first to report on a finding of celadonite (glauconite) in the paleo-weathering crust of Estonia. Isochemical weathering processes prevailed in the saprock part of the weathering profile. The studied paleo-weathering crust has also undergone diagenetic-metasomatic K-alteration during post-weathering evolution.

The mechanically weak part of the paleo-weathering crust in the Vihterpalu drill core includes paleosol, saprolite and upper saprock. The most significant weakening of the rock is related to the development of micro-fissures and loss of structural integrity during the primary stages of weathering.

Annotatsioon

Lõputöös käsitletakse Vihterpalu F332 puursüdamikust pärit kristalse aluskorra Neoproterosoikumi paleo-murenemiskooriku geokeemilisi ja geotehnilisi omadusi. Huvi taoliste komplekside parema iseloomustamise vastu on viimasel ajal suurenenud tänu mitmetele perspektiivsetele süvainfrastruktuuriprojektidele. Vihterpalu piirkonna kristalse aluskorra paleo-murenemiskoorik asub ligikaudu 200 m sügavusel ja seda katavad Fanerosoikumi settekivimid. Sealne paleo-murenemiskoorik on arenenud ränivaestes magnetiidirikastes amfiboliitides.

Uuringu jaoks koguti paleo-murenemisprofiilist 23 proovi. Kõiki proove analüüsiti röntgendifraktsiooni ja röntgenfluorestsentsi meetodite abil iseloomustamaks murenemisprofiili keemilisi ja mineraloogilisi variatsioone. Lisaks valiti kaheksa proovi geotehniliste katsete jaoks, et määrata parameetrid nagu punktkoormuse indeks, terade tihedus ning poorsus. Valitud proovidest teostati ka mikroskoopilised uuringud.

Tulemuste põhjal tuvastati murenemisprofiilis kolm osa: paleomuld (1.0 m), savirikas horisont (4.0 m) ja aluskivimid (29.0 m). Ülemise punase paleomulla horisondi moodustab äärmiselt murenenud kivim, mille CIW ja CIA murenemisindeksite väärtused on > 90. See kompleks koosneb suuresti kaoliniidist, hematiidist, illiit-smektiidist ja illiidist. Rohekat savirikast horisonti iseloomustab kompleksne sekundaarsete Fe-Mg-rikaste savimineraalide kooslus. Iseloomulikuks on savimineraali tseladoniidi esinemine (sisaldus kuni 17%). Uuring on esimene omataoline, mis kajastab tseladoniidi leidmist Eesti paleo-murenemiskoorikus. Murenemisprofiili alumises vähem murenenud osas valitsesid isokeemilised murenemisprotsessid. Paleo-murenemiskooriku savikas horisont on murenemise järgsete diageneetilis-metasomaatiliste protsesside tulemina rikastunud kaaliumiga.

Murenemiskooriku mehhaaniliselt nõrkadest kivimitest koosnev osa ulatub ligi 20 m sügavusele aluskorra ülemisest piirist ning hõlmab paleomulla, savirikka horisondi ja aluskivimi läbilõike ülemise osa. Kõige olulisem kivimite tugevusomaduste langus toimub suhteliselt vähe murenenud kivimis samaaegselt mikrolõhede ilmumisega lähtekivimi mineraaliterades.

Introduction

A paleo-weathering crust in Estonia was a product of intense weathering and erosion of the crystalline basement during the end of the Proterozoic when Earth's environment and atmosphere faced significant changes (Liivamägi *et al*., 2014). The crust forms the upper section of the Precambrian crystalline basement, below the unconformity surface between the basement and Ediacaran terrigenous complexes. The depth of the paleo-weathering crust varies from 100 m to 780 m since the surface of the Estonian basement dips southward (Soesoo *et al*., 2004). The thickness of the weathered zone can usually be several dozen metres and reach more than 100m in rare occurrences (Liivamägi *et al*., 2014).

The mineralogy and genesis of Estonian paleo-weathering crust have been addressed by the number of studies (Kuuspalu *et al*., 1971; Vanamb *et al*., 1980; Vanamb & Kirs, 1990; Liivamägi *et al*., 2014; Liivamägi *et al*., 2015; Driese *et al*., 2018). Recent studies have focused on analysing the mineralogy and geochemical composition of the paleosols to interpret ancient paleoclimate and paleogeography.

There is very little information available, however, on geotechnical properties of the Estonian paleo-weathering crust (Suuroja *et al*., 2020). It is well known that geotechnical properties could be challenging in modern weathering systems due to abrupt variations in strength, permeability and plasticity characteristics in different weathering horizons (Townsend, 1985). The interest toward a more versatile characterization of the ancient weathered complexes has appeared due to perspective deep-infrastructure projects in Estonia. At the moment, there are two projects -- Pakri hydro pump-accumulation and Tallinn-Helsinki tunnel -- station under consideration, which development foresees penetration of paleo-weathering crust. Furthermore, exploration of deep deposits such as Jõhvi magnetite quartzite also requires a better understanding of the physical-chemical behaviour of ancient weathered complexes. The available data suggest that weathering crust's geotechnical characteristics are by far less predictable than that of the crystalline basement. Furthermore, the paleo-weathering crust characteristics are dependent on parent rock type (Vanamb *et al*., 1980).

The purpose of this study is to record and explain the links between the geochemical and mineralogical properties and the changes in the geotechnical characteristics of the paleo-weathering crust from the Vihterpalu F332 drill core. The Vihterpalu F332 drill contains metamorphosed ultramafic rocks, which are relatively uncommon in Estonian basement. The weathered crust there evolved on pyroxene amphibolite and metaultrabasite complexes (Kivisilla *et al*., 1999). Being originally SiO_2-poor and Mg-Fe-rich and containing some cataclased intervals, these rocks should have been highly susceptible to weathering and mass loss.

The information gathered by the study helps to develop a more in-depth picture of the paleo-weathering crusts of the Estonian crystalline basement and to facilitate future geotechnical explorations for deep-infrastructure projects.

1. Weathering processes and weathering crusts

1.1. Weathering types and causes

Weathering crusts form during the terrestrial weathering of primary rock. In the cause of weathering the original mineral material breaks apart, and the primary rock-forming minerals are gradually lost from weathering profiles, and secondary minerals appear (Wilson, 2004). Weathering can be caused by many processes or a combination of them, and those processes are divided into two main categories: physical and chemical weathering.

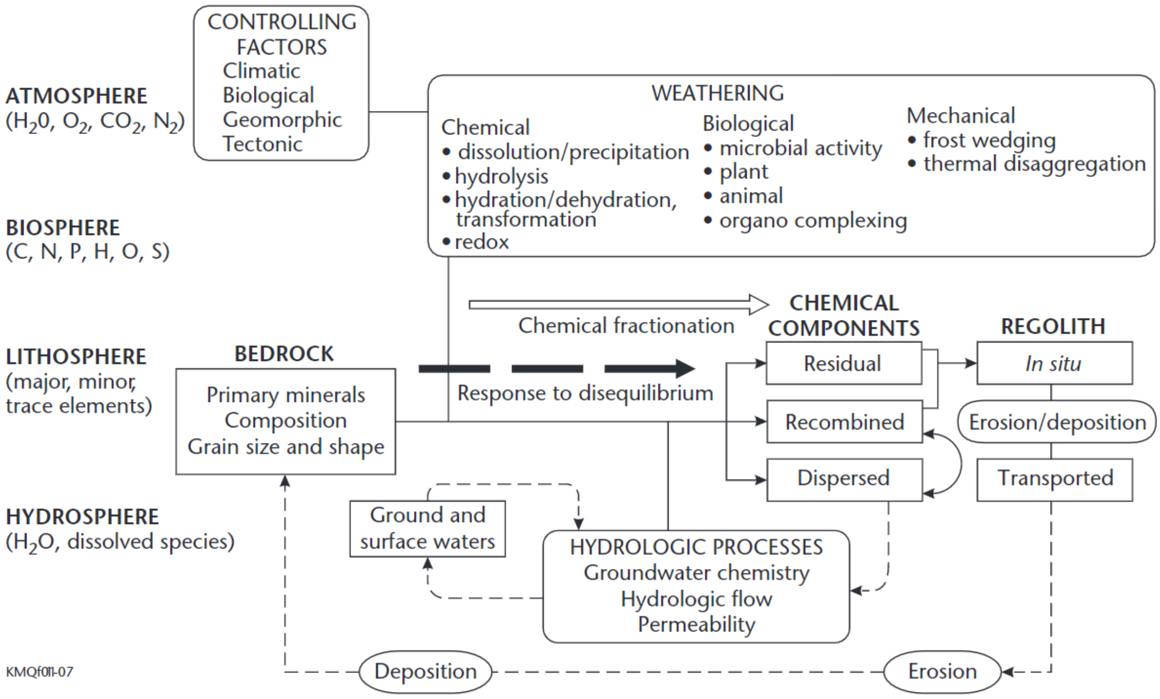

Figure 1. Main environmental factors and processes which affect the development of weathering crust (from Scott & Pain (2009)).

The process of physical weathering in principal causes the rock to break apart or crumble due to temperature changes, which can be assisted by water.

The process of chemical weathering involves chemical reactions that break down the rock-forming minerals. Mineral stability during weathering is related to its crystallization temperatures (Wilson, 2004). The felsic minerals forming at lower temperatures of the Bowen's reaction series such as quartz, muscovite, and K-feldspar are less susceptible to weathering compared to mafic minerals. Another way to determine the resistance of a mineral to weathering is the ratio of silica to other cations in its structure (Scott & Pain, 2009). As mentioned before, mafic minerals are more susceptible to weathering than felsic minerals, because mafic minerals have a higher proportion of cations that can be replaced by hydrogen ions (Parker, 1970).

Meteoric water with low dissolved ions, high molecular oxygen and CO_2 content, is chemically more aggressive than ground-water and will thus speed up the mineral alteration process. A constant inflow of water with low mineral and CO_2 content is needed for progressive weathering. Therefore intensive weathering processes are confined mainly to the zones, which are located above the groundwater level and have good drainage. The extent of weathering depends significantly on the landscape elevation -- generally reaching deeper and evolving faster rates in higher ground settings than at lower altitudes.

Climate can have a significant effect on physical weathering, especially when involving high-temperature fluctuations when the water seeps in the rock cracks and alternately freezes and thaws until the rock breaks apart. Chemical weathering is most intense in climate zones with high annual rainfall and temperature. The more water flows through the fissures and fractures, the more dissolution occurs, and with higher temperature, more components can dissolve in the water.

Weathering mostly happens in the micro-fissures and capillary systems of the rock (Wilson, 2004). Physical weathering causes the formation of those fractures and micro-fissures and gives way to the development of capillary systems. Water mediates the process of chemical weathering in capillary systems. Primary fractures and disturbances in rock could strongly influence the speed and the extent of weathering, as these features provide transport routes for infiltrating meteoric solutions.

1.2. Weathering profile

The weathering intensity and the alteration of the mineralogical and chemical properties of the rock, decrease with increasing depth.

Mass transfer processes and the development of complex zonation in mature weathering profiles depend on the mobility of major and trace elements. Chemical elements are usually divided into mobile elements (e.g. Ca, Na, P, K, Sr, Ba, Mg, plus sometimes Si) and, immobile elements (e.g. Al, Fe, Ti, Zr) (Middleburg *et al*., 1988). Immobile elements-, such as Ti, Al, and Fe, tend to get gradually enriched in the weathering crust, while the progressive loss of mobile elements occurs due to chemical weathering. Immobile elements may be preserved via original less-soluble accessory minerals ore accumulate via new supergene minerals (mainly clay minerals, oxides, and hydroxides) during weathering. Least mobile elements' contents in weathering crust could be to evaluate the alteration intensity and maturity of the regolith.

The well-evolved weathering profile is divided into three sections: soil, saprolite, and saprock. The soil, from the upper-most section of the profile, contains the most weathered material. The primary features of the parent rock are not recognizable on this horizon. It may contain some primary felsic minerals such as quartz, muscovite and K-feldspar depending on the composition of the parent rock (Wilson, 2004). Quartz is exceptionally resilient and, in some cases, can be the only recognizable mineral from the original rock in this section with the rest of the minerals having been replaced by secondary phases. The primary minerals have been replaced by secondary clay minerals making the soils very clay rich formed by the weathering of pyroxenes, amphiboles, or feldspars. Presence of iron oxyhydroxides, such as goethite, in intensely weathered complexes gives the soil a typical red-brown-yellow colour. Water is mainly free-flowing or gravitational in this part of the weathering crust, seeping downwards into the ground. Since the meteoric water contains more oxygen than typical groundwater, it will also be more oxidizing compared to the latter (Wilson, 2004). The speed of weathering is fastest here of all the zones.

Saprolite occurs in the middle section of the deep-weathered profile. Some features of saprolite show visual alteration, but the chemical composition and texture of saprolite are still comparable to these of the parent rock. The mineral variability in saprolite might be the highest in the weathering profile since the horizon still might contain some primary minerals besides the new weathering products. In this zone, pervasive weathering spreads through crystals of primary minerals and water starts moving in more prominent fissures and fractures.

Saprock is the lowest section of the weathering profile. It gradually grades into the original rock and thus has the closest resemblance to the original rock visually. The weathering processes in this zone are mostly chemical alteration reactions since temperature differences of the atmosphere have the least effect here. The first minerals here to give way to weathering are iron-bearing minerals that will start to oxidize in the water (Scott & Pain, 2009). This will create micro-fissures and capillaries through which the weathering can penetrate further on (Scott & Pain, 2009). The minerals with a higher content of Ca and Mg will also begin to transform. The quick way to assess the overall alteration rate is to observe the size of feldspars in the weathering profile, which will get smaller towards the surface. In upper saprock, the feldspar minerals will have started weathering clay minerals such as illite and smectite.

Depending on the intensity and type of alteration, a weathering profile is classified in several ways (Scott & Pain, 2009).

Beside modern weathering profiles, paleo-weathering crusts exist on shields and old stable platforms that may date back to the Precambrian. The rare, well preserved ancient paleo weathering crusts have been protected by later Proterozoic or Phanerozoic sedimentary cover. Among similar cases of paleo-weathering crusts is the Precambrian paleo-weathering crust from the north-western part of the East European Platform (including Estonia) and Ukrainian shield (e.g., Driese *et al.*, 2017). For example, on the East Russian Platform in the Republic of Tatarstan paleo-weathering crust, which is buried under 1500-2500 metres of sedimentary cover, can reach more than 50 metres in thickness (Sitdikova *et al*., 2015).

In areas where bedrock is outcropping on the surface, ancient weathering crusts have not been preserved. The genesis of paleo-weathering crust presumably share similar features with the processes that happen in modern weathering profiles. The classifications used for these complexes are derived mainly from up-to-date examples.

Nevertheless, these crusts have formed under different environmental conditions compared to the modern analogues, including distinct O_2 and CO_2 concentrations in the atmosphere and paleogeographic situations. Modern weathering is also influenced by biological processes that include microbially induced leaching and precipitation of secondary minerals and the lifecycle of land plants and soil animals (Wilson, 2004). However, for Proterozoic weathering settings, such influences are considered far less significant due to lack of land vegetation and terrestrial animals (Liivamägi *et al*., 2015).

By the end of the Proterozoic Era, primitive soil-forming processes had presumably begun on land due to biocrusts' presence. Driese *et al.*, (2007) analysed weathering and mineral alterations of feldspar, biotite, and amphibole in Palaeozoic and modern-day soils. They concluded that the differences between modern and ancient settings were not significant, apart from the impact of biota on modern-day weathering. The term "paleosol" is commonly applied for Proterozoic weathering crusts, which contains signs of primitive soil-forming processes.

2. Geology of the study area

2.1. Geology of the crystalline basement of Estonia

Estonia is located on the southern edge of the Baltica Shield. Its Proterozoic crystalline basement is coated by a thin complex of Neoproterozoic and Lower-Palaeozoic sedimentary rocks. The surface of the crystalline basement is tilted towards the south with a decline of 0.1-0.2° -per 2.0-3.5 km (Soesoo *et al*. 2020). The depth of the crystalline basement varies between 100 m to 780 m. The Estonian basement is part of the Svecofennian orogenic system which formed in 1.9-1.8 Ga as a result of subduction-related island arc collisions (Bogdanova *et al*., 2015). The Fennoscandian rapakivi granite and plutonic rocks are dated back to 1.65-1.54 Ga (Rämö *et al*., 1996).

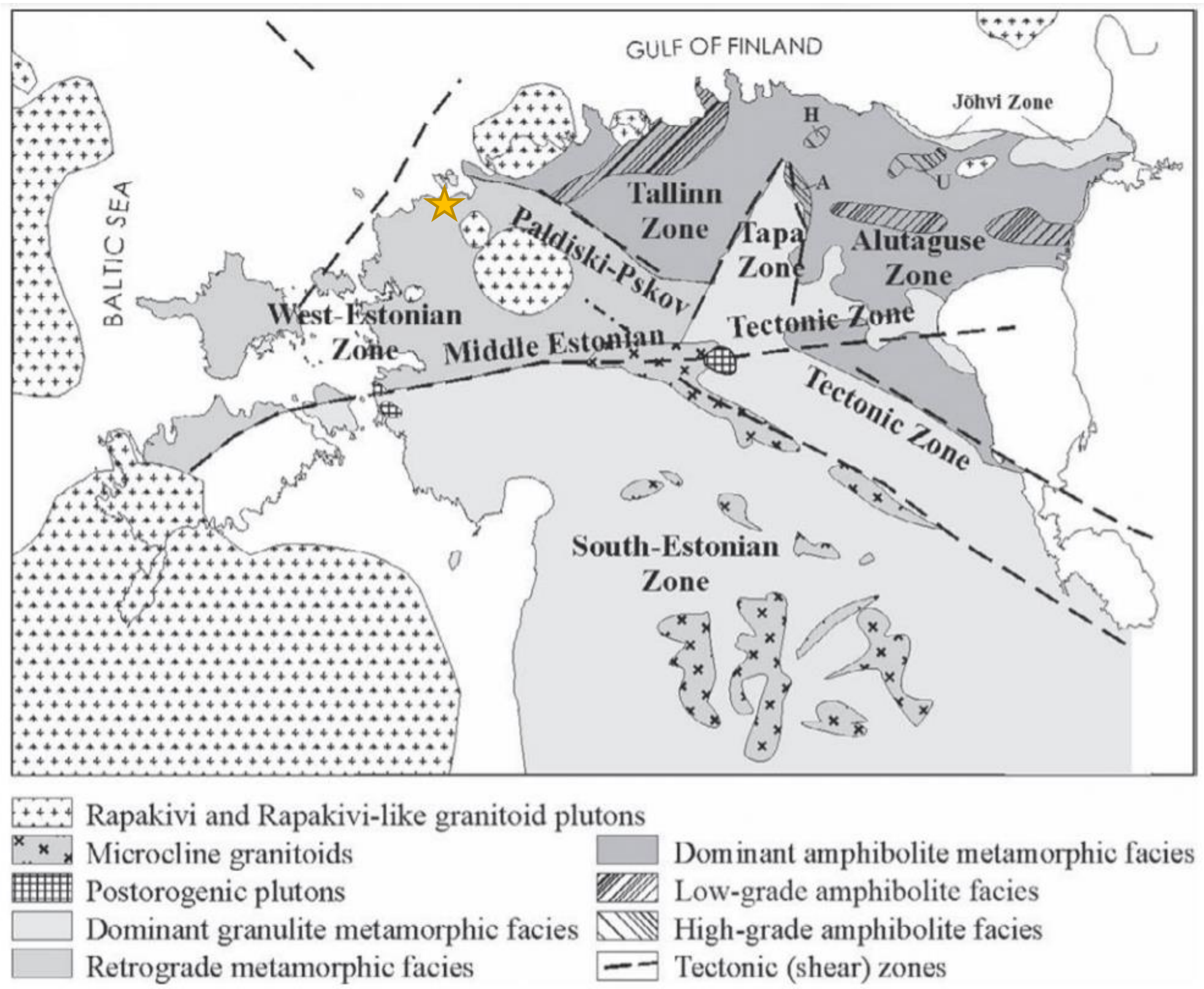

Figure 2. Main structural zones of the crystalline basement from Soesoo *et al*. (2020). A star marks the location of the Vihterpalu F332 drill core.

The metamorphic rock complexes of the Estonian basement rocks fall into two metamorphic faces by their metamorphic grade. In North-Estonia amphibolite facies rocks dominate. In South-Estonia basement is made up of high-grade granulite facies rocks. The Paldiski-Pskov tectonic fault separates these two zones (Soesoo *et al*., 2020). Six structural-petrological zones can be distinguished among the basement rocks of Estonia when taking into account geophysical and petrological studies (Puura *et al*., 1997). In the Tallinn, and Alutaguse zone, rocks formed under amphibolite facies conditions. In the Tallinn zone, acid, intermediate, and basic igneous rocks are equally widespread, whereas in the Alutaguse zone metasediments prevail (Niin, 2002). The South-Estonian, Tapa, and Jõhvi zones have formed under granulitic facies conditions. The South-Estonian and Tapa consist dominantly of basic, and intermediate igneous rocks. The Jõhvi zone, however, is relatively narrow and fragmented and shows complex rock types, including magnetite-quartzite and pyroxene gneisses (Niin, 2002). In the West-Estonian zone, the basement complexes are dominated by metasedimentary rocks, which were metamorphosed under amphibolite to granulite facies conditions (Soesoo *et al*., 2020).

2.2. Estonian paleo-weathering crust

The Estonian paleo-weathering crust was formed in Neoproterozoic between 600-560 Ma and is despite its age, remarkably well preserved. The thickness of the paleo-weathering crust can reach over 100 m, and the kaolinite-rich crust up to 40 m (Liivamägi *et al.,* 2015). In fractured fault zones, the thickness can extend to 150 m (Vanamb & Puura, 1983).

Estonian paleo-weathering crust was researched by Vanamb and Puura (1983). They classified observed weathering profiles based on spatial and structural features into three groups: fractured, intermediate, and areal weathering crust. Furthermore, the weathering profiles, based on the degree of weathering, fall into four categories – 0, I, II, and III. According to Vanamb *et al*. (1980), kaolinite is the dominant secondary mineral in the clay fraction of the Estonian paleo-weathering crust. Other common minerals in clay fractions include montmorillonite-illite, illite, chlorite, montmorillonite-chlorite, and montmorillonite. The presence and abundance of these minerals vary depending on the original rock's composition and between different horizons of a weathering profile.

The preservation of the extensive paleo-weathering crust in Estonia suggests the area was a flat terrestrial district with slow denudation in late Neoproterozoic (Puura *et al*., 1983). Liivamägi *et al*., (2015) interpreted these weathering profiles via oxisolic paleosols. Their research indicates that the thick kaolinite-rich weathering crust might have formed under tropical climate conditions. However, between 600-550 Ma, the Baltica continent was located near 55 ° to 30 ° latitudes in the southern hemisphere (Merdith *et al*., 2017). Liivamägi *et al*. (2015) proposed that multiple other factors could have facilitated intensive weathering processes, such as periods of global cooling events also called “snowball Earth” (Harland, 2007), which would have been come after by warm and humid periods (Pierrehumbert *et al*., 2011). Also, large fluctuations in Earth's CO_2 levels (Rothman *et al*., 2003), and a rapid rise in oxygen levels in the atmosphere (Holland, 2006), could have further triggered intense weathering.

2.3. Crystalline basement in Vihterpalu area

The current study is based on the paleo-weathering crust from the Vihterpalu F332 drill core. This study area is located in the West-Estonian zone. Detailed research of the crystalline basement was executed during the 1980s by the Geological Survey of Estonia in the considered region (Suuroja *et al*., 1987). The basement of the West-Estonian zone consists of rocks showing retrograde mineral assemblages. Amphibolites, biotite-plagioclase gneisses, and quartz-feldspar gneisses with minor pyroxene gneisses are the most frequent rock types in this zone (Soesoo *et al*., 2020). The amphibolites commonly form layered bodies that are intercalated with gneisses (Puura *et al*., 1997). There are two rapakivi plutons near the Vihterpalu area: the southeast and the Tallinn zone to the northeast. The eastern edge of the West-Estonian zone is edged by the Paldiski-Pskov tectonic zone, which continues in the southeast direction, and from the south, it is bordered by the Middle-Estonian tectonic zone.

The Vihterpalu F332 drill core is 326.5 m long. The thickness of the sedimentary cover is 203.6 m, and the latter is made up of Ediacaran to Ordovician sedimentary rocks and Quaternary sediments. The crystalline basement in the Vihterpalu drill core comprises various metamorphic complexes (Suuroja *et al*., 1987). The recorded rock types are pyroxene amphibolite, diabase, amphibolite, granodiorite, amphibolite-biotite gneiss, and granite. Cataclastic features and migmatization are widespread in some parts of the section. The upper part of the basement in which the weathering crust has evolved consists of magnetite-rich amphibolites. These rocks are distinguished by porphyroblastic texture and massive structure, disrupted by cataclastic deformations, sliding surfaces, and irregular carbonate-bearing veinlets.

The rather low SiO2 (commonly < 45.0%), high iron, and magnesium content of these rocks (Kivisilla *et al*., 1999) suggest an ultramafic to the mafic precursor. According to Suuroja *et al*. (1987), the primary assemblages were formed as volcanogenic or hypabyssal complexes. The reported mineral assemblage of the magnetite-rich amphibolites is plagioclase (28.4-51.9%), hornblende (39.2-49.9%), pyroxenes (up to 25.7%), biotite (up to 8.5%), opaque Fe-phases, quartz (up to 4.8%), titanite (up to 0.7%), epidote (up to 4%) and carbonate minerals. Retrograde amphiboles commonly replace primary pyroxenes in these rocks.

According to the original drill core description, the thickness of the paleo-weathering crust in the Vihterpalu drill core was determined to be 30.4 m (Suuroja *et al*., 1987). In nearby drill cores weathering crusts with the following thicknesses have been found: Vihterpalu 357 21.0 m, Ristna F331 29.4 m, Englema F333 6.5m, Hatu F336 9.0 m (Kivisilla *et al*., 1999). The Ediacaran clastic sediments from the Gdov Formation overlie the weathered crystalline basement in the area.

3. Material and methods

The Vihterpalu F332 drill core is owned by the Geological Survey of Estonia. Its major geological information could be found in the database of the Estonian Land Board (https://geoportaal.maaamet.ee/index.php?lang_id=1&action=viewPA&GB_id=6242AK_0003&fr=o&bk=1&page_id=382).

Prior to sampling, visual examination of the profile was conducted along with photographing of the core boxes. It was determined that the weathering crust (based on macroscopically identifiable features) extend from 204 m to 233 m, which agrees with previous descriptions by Suuroja *et al.* (1987). Some intervals from the upper few metres of the weathering crust suffered from a poor core recovery.

The samples were collected roughly in 1 m to 2 m intervals to represent significant lithological variations along with the weathering profile. A quarter of the drill core was used for sampling. Sample length varied between 4 cm to 14 cm. Altogether, 23 samples were taken from the core section.

The samples were then coded and separately photographed with a ruler for size reference. Before geotechnical and laboratory analysis the samples were also colour coded with Munsell's soil colour chart (Munsell's Soil Colour Book, 2012). A sample colour was determined with 2 to 3 colours, to which additional colours of veins or local irregularities were recorded.

Out of the 23 samples, eight were chosen for thin section preparation. The distance between the selected rock samples varied from 3 m to 8 m. In some cases, intervals were longer since a few of the samples in the upper section were very brittle or already crumbled and were not suitable for thin section preparation. The thin sections were made on 7.5x2.5cm glass slides. The glue used for this process was Petropoxy 154. Some of the samples had to be saturated with glue before mounting on the glass slides. It helped to ensure the integrity of the weathered rock during thin section preparation. The thin sections were analysed and photographed under the polarizing microscope.

After thin section preparation, geotechnical tests were performed on eight samples. The intervals between the chosen samples varied from 2 m to 9 m. The geotechnical testing consisted of point load tests, porosity tests, and volume measurement tests.

Point load measurements were conducted first since these required larger intact samples. As the sample sizes were relatively small, measurements could only be repeated 4-6 times.

Sample porosity and volume were measured with a single test, which consisted of several procedures. First, the samples were heated for a few hours to get an accurate measurement of the oven-dry rock. After this, rocks were placed in the bottom of a cylinder, full of water and had a water column height of around 1.0 m. The rocks were left in the water for a few days so the pores would get saturated with water. The weight of rocks was then measured both in water and in dry air with the saturated pores. Some of the samples crumbled a bit during measurements and thus had a more significant variation between dry to saturated measurement.

For all 23 samples, X-ray diffraction (XRD) and X-ray fluorescence (XRF) analysis were conducted. The bulk samples were crushed and ground into a fine powder and then further prepared for the analysis. To determine the key components, fused samples were made for XRF analysis by mixing a ground sample with a borate flux, heating, and then casting a molten sample into a homogenous flat disc. The samples were analysed with a Bruker S4 spectrometer using Bruker's pre-calibrated MultiRes measurement method. For XRD studies, powder samples were measured with the Bruker D8 ADVANCE diffractometer (Co tube) with a Lynxeye detector. XRD patterns were analysed with the TOPAS software using Rietveld refinement to obtain a semi-quantitative mineral composition. All sample preparation procedures and laboratory analyses were conducted in the laboratories of the TalTech Department of Geology by the author, except for XRF and XRD analyses, which were conducted by the lab staff.

4. Results

4.1. Lithologic description of the weathering profile

Figure 3 shows the location of samples and primary lithologies of the studied section. The first uppermost samples of the weathering crust (from depth 204.1-204.2 m) have a dusky red colour, are visually quite similar, consisting of a uniform, dense fine-grained material without original lithic fabric and exhibiting characteristic laminated structure. The samples belong to the paleosol zone. The two following samples (205.5-206.0 m) are characterized by a heavily weathered fragmented rock in which original lithic fabric could be sporadically recognized. Samples colour transitions from dark red to light shades of green. The next samples (205.0-209.0 m) are more or less compact, weathered amphibolite showing mostly greenish tones, mixed with red, brown, and grey. They also contain a network of crosscutting light-coloured carbonate veinlets. In some samples breakage of drill core has occurred along these veins. The thickness of the individual vein is not more than 1 - 3 mm. The strength of the rock from this interval varies but is somewhat lower compared to the rest of the weathering profile, —the rock can be broken into smaller pieces without difficulty. The mineral crystals in this horizon are too small to distinguish specific features on a macroscopic scale. In situ formed secondary minerals prevail in the mineral assemblage. The following section (210.0-215.0 m) comprises of stronger compact weathered rocks. It is possible to isolate primary minerals within the rocks, and the samples have preserved lithic fabrics of parent rocks, but the rock is still heavily weathered, especially in the first two of the samples. The samples contain carbonate veinlets, but they are not as abundant as in previous samples sets. In some samples, small brown-red fractures coated by iron—phases appear. In one sample, a distinct half-centimetre-thick green alteration rim was recorded around a thick red-brown fracture. The colour of the samples generally varies from green to blackish grey, accompanied by shades of red. The sample from 216.3- to 216.4 m contains fractured, fragmented pieces of heavily altered amphibolite, which hosts white calcitic veins. Below this interval signs of weathering become less pronounced in the core. In the next section (218.0-223.0 m), the samples begin to resemble the original rock due to its textural features and strength. The colour is mostly black dark, dark grey or dark green. The veins in this interval tend to be less prominent. The red colour from secondary iron minerals can still be visible in some samples. The porphyroblastic textures of the parent rock are better preserved, making the edges of the crystals more detectable. The last studied section (225.0-237.0 m) can be described as the transition zone from saprock to the original rock. The samples still present some visual signs of weathering especially in 233.0 m, the macroscopic traces are mainly restricted to small red-brown fractures that occasionally penetrate the rock and narrow alteration zones around the fractures, which is similar to the one previously described in the 210.0-215.0 m section. The lowermost sample (237.1-237.2m) has a visual appearance similar to that of the un-weathered amphibolite.

4.2. Mineralogical composition and microscopic description

Mineralogy of the Estonian paleo-weathering crust has been previously analysed by Kuuspalu *et al.*, (1981), Liivamägi *et al*. (2015), and Vanamb & Kirs (1987). The earlier works focused solely on the clay fraction of the weathering profile. The mineralogy of the whole rock samples was determined by XRD analysis and microscopic studies in the thesis at hand. The results of XRD data are found in appendix 1.

The mineralogical analysis helped in dividing the weathering profile into three zones: paleosol, saprolite, and saprock (upper saprock and lower saprock). The top portion of the weathering crust or paleosol composed mainly of secondary clay minerals, with kaolinite accounting for the majority (ca. 40%), followed by hematite (ca. 25%), and other clay minerals (illite-smectite, smectite, cordierite)(ca. 30%). The primary minerals of the parent rock were completely lost from this horizon due to the extensive weathering (except quartz, which occurs in trace quantities) leading to the development of impoverished secondary mineral assemblage. Beside iron oxides, secondary titanium oxide anatase is enriched in the paleosol horizon. In the clay-rich saprolite section, more diverse mineral associations can be distinguished. The content of ferruginous minerals is considerably lower, but secondary phyllosilicates still prevail in the mineral assemblage. However, their composition differs considerably from that of paleosol. Kaolinite content has dropped below 8%, and chlorite content stays within a similar range to it. From other clay minerals, illite-smectite(I-S) dominates constituting from 30 to 60% of the weathered rock. Beside I-S some cordierite and smectite might be present, but these phases could not be reliably distinguished based on analyses. A distinct feature of the studied saprolite horizon is an occurrence of celadonite (0-17%). Celadonite is a green potassium dioctahedral mica with 1M structure and general formula $K(Mg, Fe^{2+})Fe^{3+}(Si_4O_{10})(OH)_2$ (Drits *et al*., 2010). It is structurally similar to another green mica, glauconite. No strict distinctions between these two phases are made in the study. To the best of the author's knowledge, this is the first study that reports of celadonite (glauconite) occurrence via major rock-forming phase in the Estonian paleo-weathering crust.

Beside phyllosilicates, the saprolitic horizon is characterized by the high content of orthoclase (ca. 10-15%). Hematite portion fluctuates a lot in this zone (7-15%) as does dolomite (8-22%). The portion anatase decreases downwards. This trend correlates with the appearance and increase of ilmenite. The underlying saprock horizon could be divided into two zones since the upper and lower part of this section show significant differences. Secondary minerals celadonite (glauconite) and dolomite almost disappear in the transition to saprock. Their disappearance coincides with the appearance of primary minerals, Mg-hornblende and anorthite. Content of clay minerals, anorthite, and augite in the upper section of the saprock fluctuates as do the contents of some other phases, but to a lesser extent. The proportion of kaolinite drops compared to saprolite, similarly to the transition from paleosol to saprolite. In the lower saprock section kaolinite disappears completely. Dolomite content also drops down in the transition and quite significantly. The decrease of orthoclase correlates with the increase in anorthite in the transition to saprock. The transition to the lower saprock section can be defined by the stabilization of mineral content and the disappearance of some secondary minerals, such as orthoclase and anatase. The proportion of minerals like augite and anorthite rises and becomes more stable. Since secondary clay minerals persist in the lowermost sample, even though their content says below 23%, the lower boundary of the paleo-weathering profile resides somewhat deeper than previously suggested.

Representative micro photos of studied thin sections from the weathering crust are presented in Figure 3.

The only thin section from a paleosol (from a depth 204.0 m) contains very weathered material, and no primary minerals could be detected. The grain size of the minerals in the sample is very small. The only minerals that can be distinguished are secondary iron phases, which aggregates can be 50 microns or more in size. The colours of the thin section are light yellow to brown or reddish-brown. The opaque iron minerals and iron coatings define the overall appearance of the rock. The structure of the rock varies from lenticular discontinuous wavy laminations to massive. There are many cracks in the rock evidencing brittle character of the material. There are also systems of thin veinlets visible in the thin section and colours of these veinlets can vary from black to reddish-brown.

The sample from saprolite section (from a depth 207.0 m) is characterized by massive fabrics dominated by light green and yellow secondary minerals. Although weathering is pervading, in some cases, it is still possible to distinguish the faint outlines of primary minerals, that suggest the pseudomorphic replacement of primary phases, -such as amphiboles. The larger replaced grains show a brownish-green colour and lighter green edges probably representing amphiboles replaced by Fe-rich micas. Between these greenish aggregates is a network of light to darker yellow altered grains. Black non-transparent iron oxides occur regularly scattered in the rock. Their aggregate size is similar to that observed in the paleosol. Nevertheless, the proportions of the opaque minerals stays considerably lower compared to paleosol and grains of subhedral to anhedral magnetite with sharp outlines appear.

The next thin section is from the upper saprock from a depth 214.6 m. Minerals in this thin section show considerably fewer signs of intensive weathering and weathering features are irregularly distributed in a centimetre-scale. The minerals and textures inherited from the host rock define the overall appearance of the sample. There are two phases easily distinguishable in this sample. The olive-green hornblende forms large porphyroblast, which contains scattered Ca-plagioclase crystals. High-temperature mafic minerals show different degree of alteration varying from completely replaced grains to slightly altered grains with the unaltered part in the middle between larger primary grains. Smaller grains develop due to intraminerals micro-fissures. Some of the cracks contain red or orange iron coatings. The distribution of magnetite grains is similar to that observed in saprolite.

The last thin section of the upper saprock is from a depth 220.7 m. The hornblende-rich thin section is mostly green, varying from light yellow to darker green. The sample shows possible cataclastic features -- primary mineral grains present mosaic-fragmented texture. In bigger grains, a dense network of fractures might show up along primary cleavage. The anorthite and augite are largely replaced by the secondary mineral phases. The aggregates of magnetite have a bigger size compared to previous thin sections and present higher abundance. There are also specks of red seen in the sample due to local irregular iron coatings on grain rims.

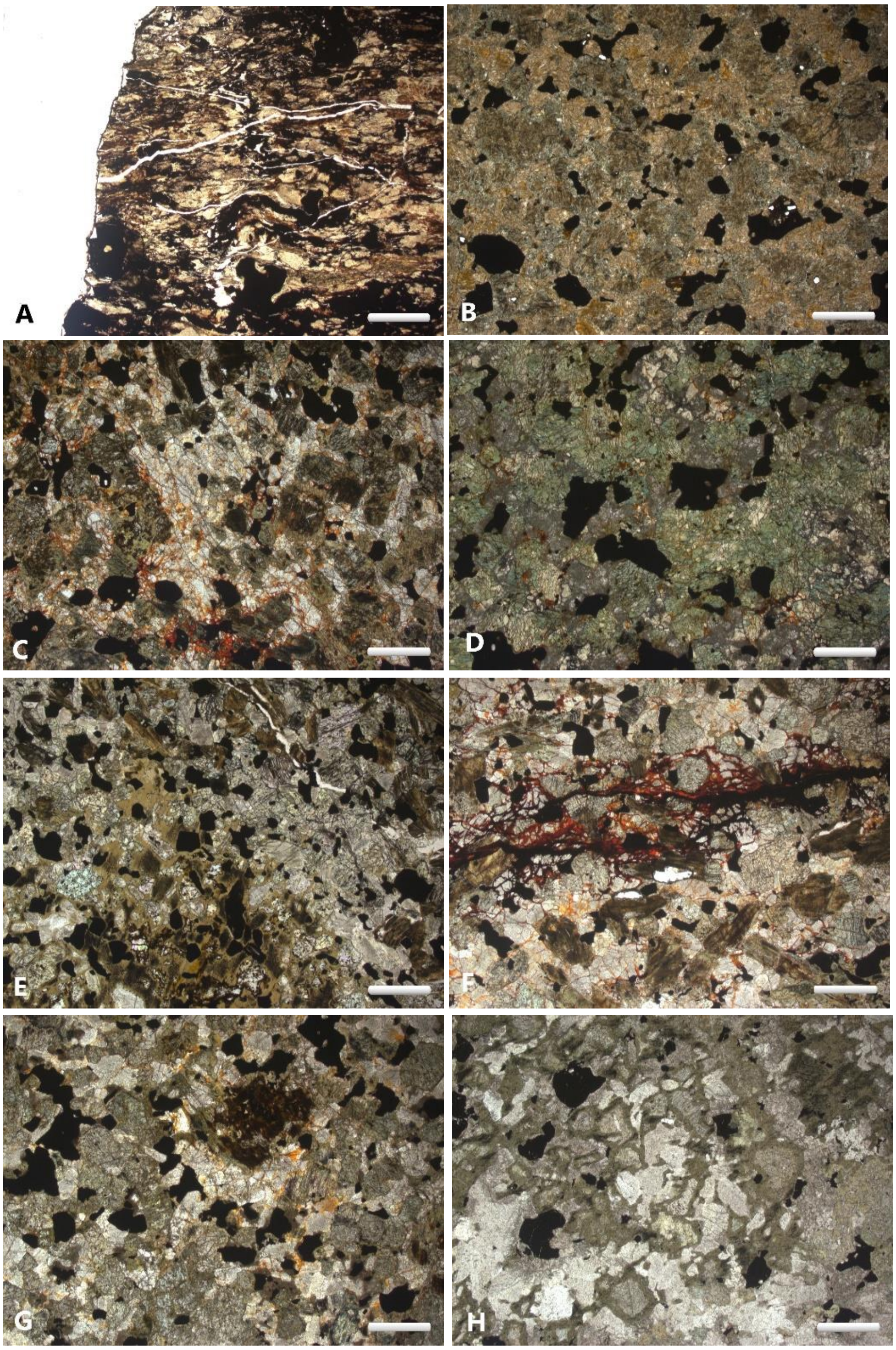

Figure 3. Images of the paleo-weathering crust in the Vihterpalu F332 drill core under a polarizing microscope. A: paleosol sample (204.1 m); B: saprolite sample (207.0 m); C-D: upper saprock samples (214.6 m, 220.7 m); E-H: lower saprolite samples (223.8 m, 227.0 m, 233.2 m, and 237.0 m)

The samples from a depth 223.8 m, 227.0 m and 233.2 m represent the lower saprock. The upper sample contains large, altered porphyroblasts of yellow-brown amphibole along with altered biotite and magnetite, which all are formed as the result of retrograde metamorphism. Light pinkish-grey grains of augite and small crystals of plagioclase could be distinguished in this sample. Unlike porphyroblasts, the two latter, typically show intragranular cracks. Minor rusty coatings on crystal edges occur occasionally. The next sample from below also shows porphyroblastic fabric, but considerably larger crystal sizes of matrix-forming metamorphic minerals such as Ca-plagioclase. Alteration is less pronounced, but it is hard to differentiate retrograde metamorphic changes from weathering effects. There was one noticeable difference from the previous sample, the more widespread presence of ferruginous coatings on grain edges and intragranular cracks.

In the sample from a depth 233.2 m, which also presents pophyroblastic fabrics, less durable primary minerals, such as plagioclase and pyroxenes, present more easily recognizable crystal morphologies and larger crystal sizes than in samples from the upper part of the profile. The alteration features are visible along grain boundaries of Fe-Mg containing primary phases and via pseudomorphic replacements of single primary grains.

The last sample from a depth 237.0 m is from the lower-most part of the studied section and presents the weakly altered part of the paleo-weathering profile. The rock is texturally and structurally rather similar to the un-weathered porphyroblastic amphibolite. Signs of alteration are confined to grain boundaries or appear as replacements of individual primary grains.

4.3. Geochemical composition

The full geochemical dataset for the Vihterpalu drill core obtained by XRF analysis is proved in Appendix 2, and variations of the selected compound are presented in Figure 4. The recorded variance ranges for the major elements in altered silicate rocks were 26.43-42.67% SiO_2, 1.12-2.89% TiO_2, 9.69-25.01% Al_2O_3, 15.26-37.07% Fe_2O_3, 0.47-11.48% MgO, 0.20-14.44% CaO, 0.02-0.88% Na_2O, 0.06-5.88% K_2O.

Elements such as Ti and Al are considered relatively immobile in typical weathering environments and can be therefore used as markers for assessing the losses or gains of other elements.

The paleosol zone is depleted regarding parent rock in mobile elements such as Mg, Na, Ca, and K, showing only trace amounts of these elements. There is a notable drop in Si content and significant rise (> 1.3 times) of Ti, Al, and Fe abundance in paleosol compared to the values in saprolite.

In the saprolite zone, the content of the most major elements fluctuates in a wide range, except that of Na, which content stays below 0.1 % until the transition to saprock. Values of Al and Si change very similarly, showing a clear positive correlation, so does the content of Fe and Ti. It could also be noted that the

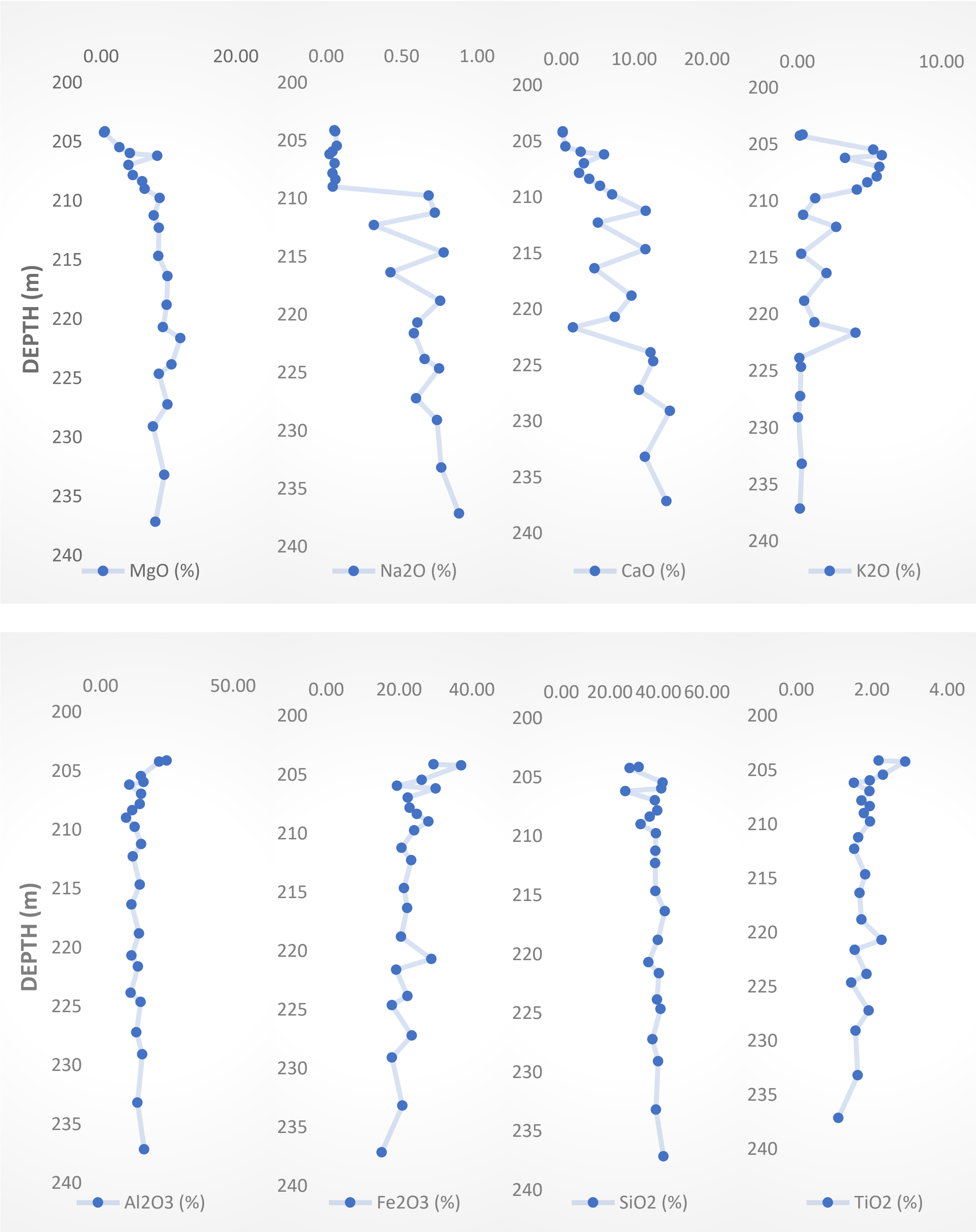

Figure 4. Results of the XRF analysis representing the change of Mg, Na, Ca, K, Al, Fe, Si, and Ti relative to depth. The depth of the analysed samples is shown on the vertical axis and element content is plotted along the horizontal axis.

values of these two element pairs change in the opposite direction when compared to each other. Notably, Ca and K abundances demonstrate a negative correlation in the saprolite samples. The post-weathering genesis of K-enrichment in saprolite is indicated by the considerable enrichment of K above regular content in the parent rock. Mg content changes similarly to Ca being highest in carbonate-rich samples. Presence of carbonate veins (samples from a depth 206.0 m) appears as abnormally high Ca and Mg values in the geochemical dataset.

In the upper saprock section, the content of Si and Al stabilizes and remains more or less constant throughout the rest of the weathering profile. Mg, Fe, and Ti content also stabilizes, but their abundance shows significant rise in the transition from saprolite to saprock. The content of Na, Ca, and K fluctuates significantly in saprolite. However, these three elements still present linked behaviour – Na and Ca exhibiting positive correlations with each other and negative correlations with K.

In the lower saprock zone, the content of Si remains very stable. Also for Mg, Fe, Al, and Ti the changes are not very significant in this horizon. However, the content of Na and Ca fluctuates considerably, whereas K content remains invariably low.

4.4. Geotechnical characteristics of the rocks

The result of the point load test, porosity and density measurements of the samples are illustrated in Figures 5-8.

The point load test results, which could be used for evaluation of uniaxial strength of the rock, show that the overall strength of the rock rises with depth. However, the standard deviations of point load indexes of test series were found to be rather large. Therefor only superficial conclusions could be drawn from the obtained results. The paleosol and saprolite zones present the lowest point load values. The lowest values in these clay-rich rocks are related to sample with the lowest hematite content, suggesting that the presence of secondary iron oxides likely plays a significant role in stabilizing these beds. The samples from the upper saprock zone show a rise in recorded point load values compared to overlying zones, but the values also fluctuate significantly. The strength of the rock from the lower saprock section is considerably higher compared to upper saprock part -- the highest point load index values reach up to 6.5 in these rocks. For statistically more reliable evaluation of these rocks' actual strength characteristics, bigger test samples are needed.

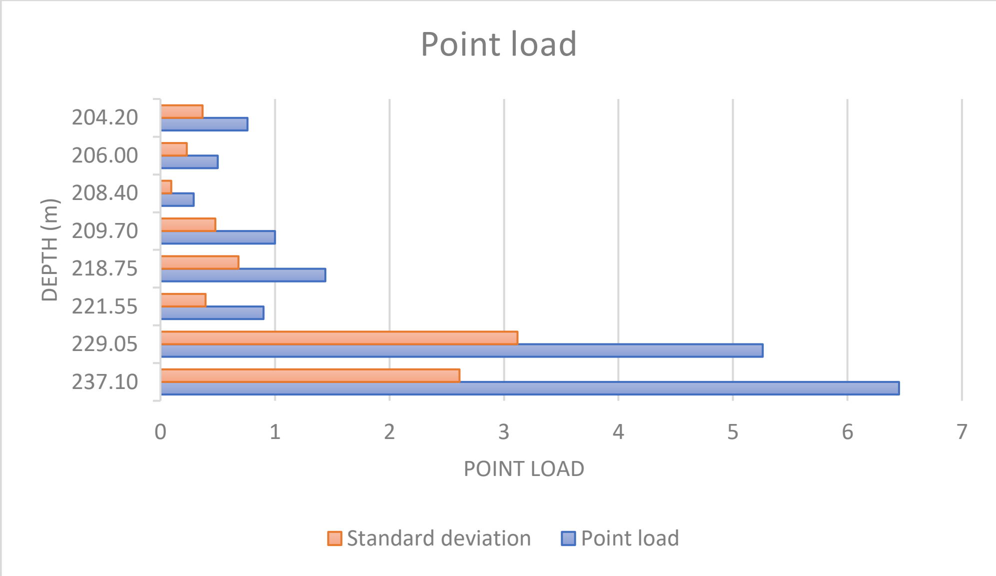

Figure 5. Bar chart of the point load index values relative to depth. Two values are shown here: orange represents the standard deviation of the point load and blue represents the point load index.

The results of the porosity measurements show that the (opened) porosity of altered rocks gradually decreases with depth in the upper part of the paleo-weathering profile. The highest porosity characterizes paleosol, reaching up to 45% of the total rock volume, followed by the two samples from the saprolite zone with porosity values slightly higher than 20%. Porosity of saprock samples was the lowest staying generally below 10% of the rock volume. The five drillcore samples in the saprock zone did not show a clear correlation between porosity and depth, suggesting that the development of secondary porosity in considered horizons was dominantly

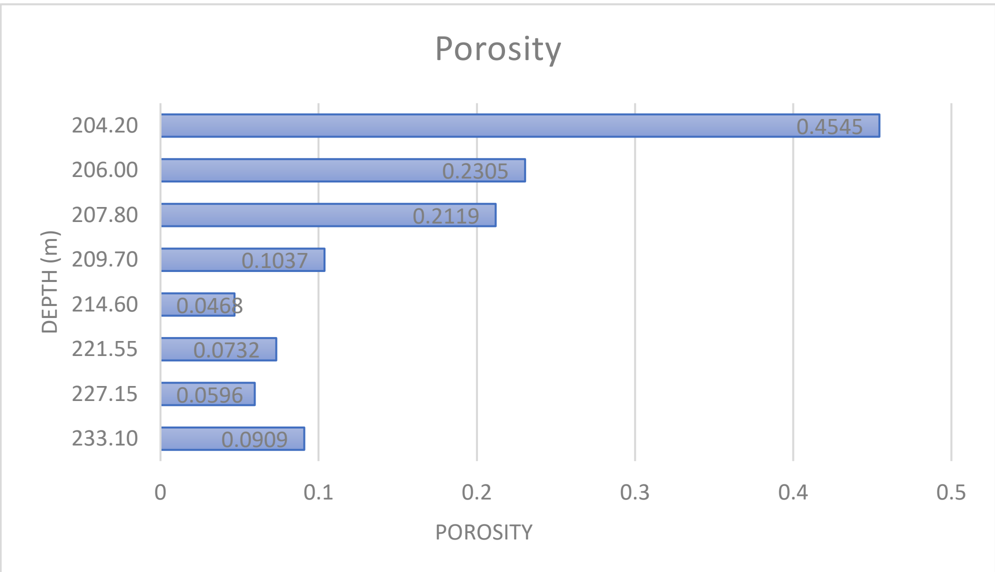

Figure 6. Bar chart of the approximate porosity values relative to depth in the weathering profile.

controlled by variations in parent rock type.

Saturated bulk density of the rock describes a sample's weight when saturated with water at room temperature. The results show that saturated bulk density of rocks from the paleo-weathering crust from the Vihterpalu drill core rises with depth. The lowest value of saturated bulk density (2168 kg/m^3) was recorded in the paleosol zone, followed by saprolite samples. Below this depth, in the saprock, the bulk density stays mostly on the same level (2973±49 kg/m^3).

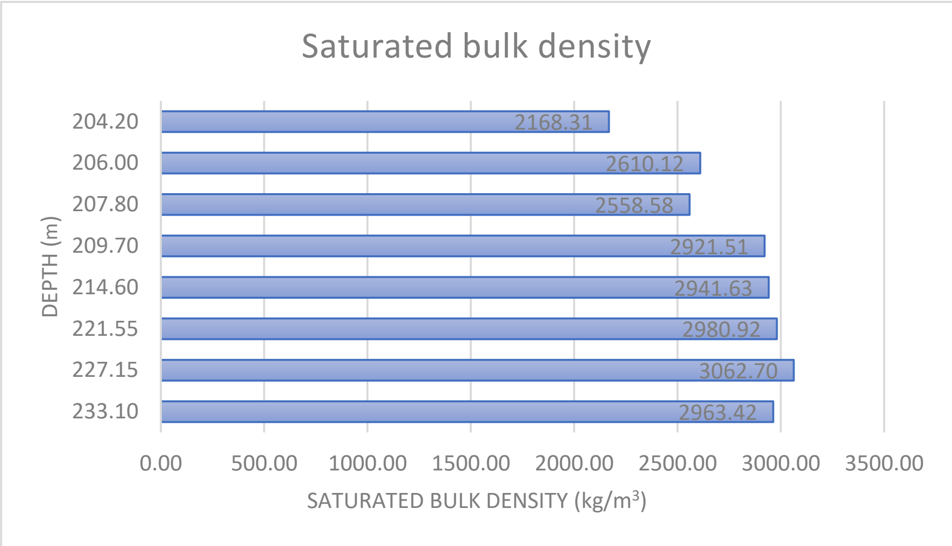

Figure 7. Bar chart of the saturated bulk density relative to depth in the weathering profile.

Grain density describes the density of solid matter of the samples, which reflect complex mineralogical variations in the weathering profile. Thus, the grain density is high in iron oxide rich paleosol and saprock samples, but shows the lowest values in more iron-poor and clay-rich samples, which are from the lower part of saprolite.

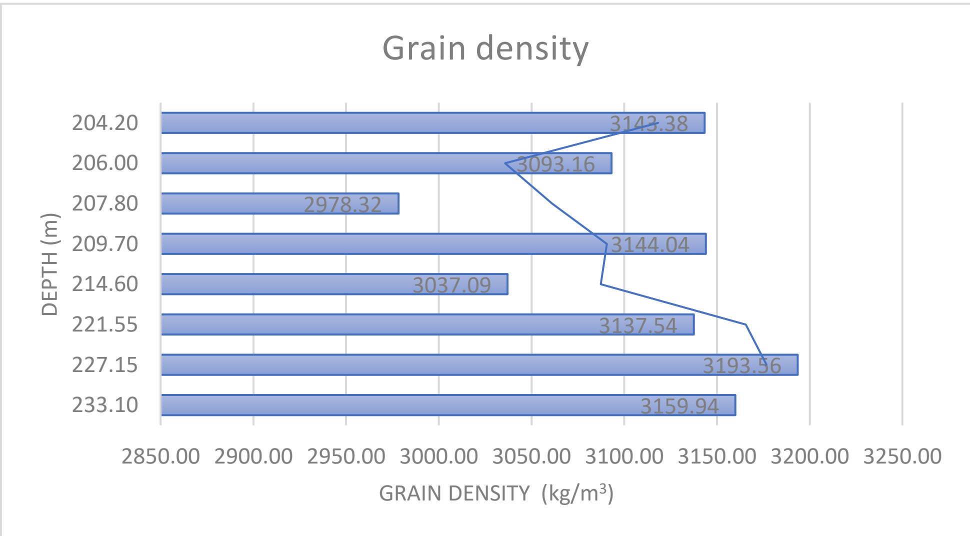

Figure 8. Bar chart of grain density relative to depth in the weathering profile.

5. Discussion

5.1. Degree of chemical weathering

To assess the geochemical changes during weathering, certain indices have been introduced to characterize mobilization and transport of chemical compounds in the weathering profile. The most widely used proxy is a chemical index of alteration

CIA= $(Al_2O_3/(Al_2O_3+CaO^*+Na_2O+K_2O))$ x100 (1)

where CaO* is Ca bound only to silicate minerals, in the molar ration (Nesbitt & Young, 1982). The second widely used parameter is a chemical index of weathering

CIW=$(Al_2O_3/(Al_2O_3+CaO^*+Na_2O))$ x100 (2)

where CaO* is Ca bound only to silicate minerals, in the molar ration (Harnois, 1988).

In both indices, the content of Al is used to measure the loss of soluble cationic compounds from the weathering profile.

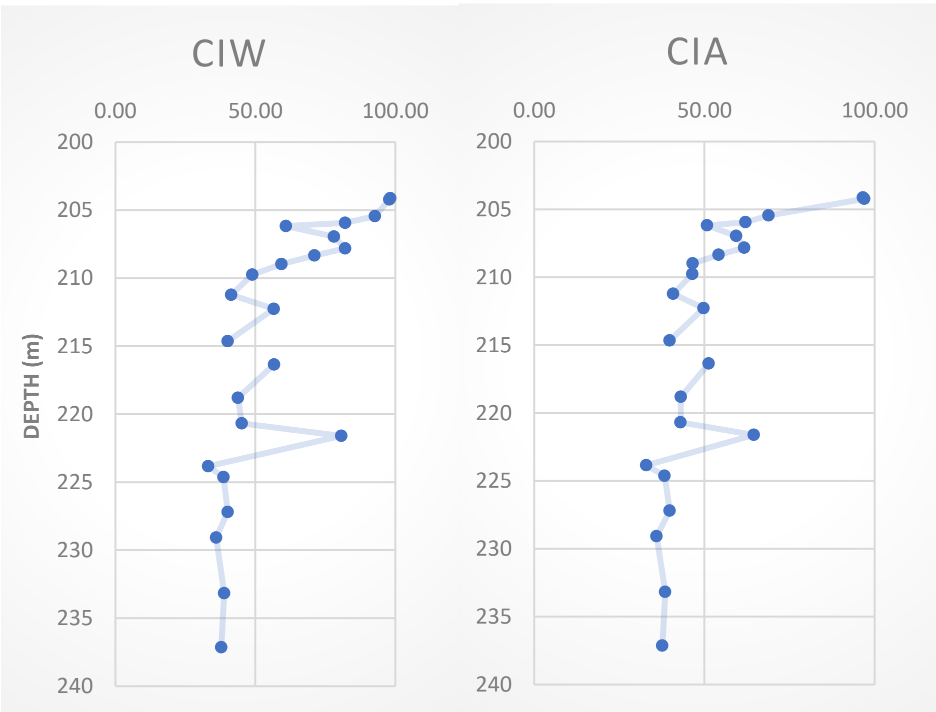

Figure 9. CIW and CIA values for the paleo-weathering crust from the Vihterpalu drill core. Calculated index values are plotted along the horizontal axis of the charts. The vertical axis shows the depth of samples.

The calculated trends are quite similar in the lower part of the profile but differ significantly in the upper part of the paleo-weathering crust. Gathered data suggests that K-diagenetic-metasomatic alteration of K abundance in the weathering crust has masked original syngenetic potassium variations in saprolite and upper saprock. K-overprint has been recorded from various clay-rich paleosols (Fedo *et al*., 1995). In the case of Estonian Proterozoic paleo-weathering crust, the K-overprinting by post-weathering processes has been demonstrated Liivamägi *et al*. (2014, 2015).

Both CIA and CIW values peak in the paleosol zone (204.1-204.2 m) staying > 96. The high values indicate that paleosol is highly depleted in labile cations. The indices record intensive geochemical weathering and removal of soluble compounds by percolating meteoric waters. Remarkably, the latter overprinting has not affected paleosol K distribution, indicating that K fixation was controlled by the character of precursor silicate phases in saprolite and saprock. The upper saprolite section starts with a significant drop in CIA value and considerably less pronounced drop in CIW values. The overall trends in this zone demonstrate a sharp decrease of weathering intensity toward the lower boundary. However, there are slight fluctuations in the calculated index values in samples showing high dolomite content. The CIA and CIW values in the upper saprock fluctuate in a range from 1 to 5. However, but no clear trend in weathering indices could be observed, suggesting that weathering intensity is first of all controlled by variations in parent rock character. The last sample in the upper saprock section (221.0 m) demonstrates a significant increase in CIA and CIW values. It relates to the more altered fractured rock section in the saprock. In the lower section of the saprock (224.0-237.0 m) the CIA and CIW values are relatively steady and show a bulk rock composition close to that of the host rock (data from the Kivisilla *et al*. (1999)). Thus, the lower part of the weathering profile has likely altered in closed system iso-chemical weathering processes.

5.2. Linkage between geochemical and geotechnical properties in the paleo-weathering crust

The study of the paleo-weathering profile form the Vihterpalu drill core, which evolved on the Mg-Fe rich amphibolite parent rock, shows the occurrence of considerably thin horizons of intensely weathered residual kaolinitic-ferruginous paleosol and Mg-Fe clay-rich saprolite. Specific for studied saprolites, is the presence of secondary celadonite (glauconite), which has developed syngentically during weathering or as the result of post-weathering alterations.

The thickness of the paleosol (ca. 1.0 m) and saprolite (ca. 4.0 m) horizons of the Vihterpalu F332 weathering profile is similar to that described by Liivamägi *et al*. (2015) form the Varbla 502 drill core. In the case of latter pyroxene, gneisses occur as a parent rock. However, the paleosol horizon has most likely undergone significant erosion before the sedimentation of the Ediacaran deposit and thus does not represent the original thickness of the soil bed.

The low silica amphibolites should have been in theory been more susceptible to chemical weathering than more acidic rocks from the crystalline basement. However, acidic complexes from the Estonian crystalline basement might present much more extensive weathering profiles (Kivisilla *et al*., 1999) and thicker saprolite horizons (Liivamägi *et al*., 2015). This suggests that the resistance to mechanical disaggregation and erosion of weathering profiles, which evolved on Si-poor and Fe-

Mg-rich rocks was likely considerably lower compared to more acidic quartz containing complexes. The limited thickness of the weathering crust might also reflect the influence of local topography to weathering processes.

According to Meunier (2005), mineral reactions in weathering profiles, which have evolved on amphibolites and ultrabasic rocks, are governed by magnesium leaching and Fe oxidization. In the paleo-weathering crust from the Vihterpalu drill core leaching and loss of Mg become evident in saprolite, while in saprock horizons only minor Mg loss could be detected. Secondary hematite appears already in the lower part of saprock and signals Fe oxidization in the weathering profile. Nevertheless, considerable Fe enrichment and abundant presence of secondary hematite are restricted to saprolite and paleosol horizons. Meunier (2005) also stressed the importance of grain size to the first weathering stages of basic coarse-grained rocks such as gabbros and amphibolites. Irregular patchy alteration patterns in weakly weathered porphyroblastic amphibolite samples from the Vihterpalu drill core section suggest the structural and textural patterns in parent rock had strong control over the alteration pathways during the first stages of alteration.

Although the mineralogy of the weathering crusts from the Vihterpalu core section presents some unique features, it still holds many parallels to weathering crusts described by earlier studies. Thus the mineralogy of the paleosol from the Vihterpalu core is very similar to other paleo-weathering crusts from the Estonian crystalline basement showing kaolinite- and Fe-oxyhydroxides-rich assemblages with an admixture of Illite-Smectite and illite (Kuuspalu *et al*., 1971; Liivamägi *et al*., 2015). However, there is almost no trace of gibbsite in the weathering profile and low chlorite content compared to the usual basic and acidic weathering profiles. Quartz content is also very low, due to the character of the original rock. The colour variations recorded from the Vihterpalu drill core match with general colour variation described in case of other Estonian paleo-weathering profiles, e.g. paleosol showing mostly red tones and saprolite being greenish-grey.

Recorded trends in the paleo-weathering profile geotechnical properties closely follow geochemical and structural changes in the altered rock. The upper kaolinite-ferruginous residual horizon is characterized by significantly higher porosity compared to the underlying sequence. The high porosity determines high groundwater content in the uppermost horizons of the paleo-weathering crust. Compressive strength of the paleo-weathering profile appears to be lowest in clay-rich saprolite horizon. It is highly likely that due to poor core recovery from this horizon and fragility of samples, the weakest rocks of the saprolite were not tested by the study. However, the weathered rocks remain considerably weak also in the upper part of the saprock profile. Sharp changes in rock mechanical strength occur only considerably deep in weathering profile -- the weathering crust seems to become relatively stable only from depth 230 m. The measured point load index values of the samples from the lower saprock are more than four times higher than those from the upper part of the saprock.

Based on the collected data, it is apparent that the prime loss of rocks strength was not linked with advanced stages of geochemical weathering. A significant decrease of rock strength instead occurred during the first stages of parent rock transformation and development of microscale discontinuities within the rock mass and reduction of the size of primary crystals.

The upper ca 20-metres-thick section of the weathering crust from the Vihterpalu core varies significantly in its geotechnical properties and should thus be treated as a potential hazard zone when planning deep-infrastructure projects.

Conclusions

The paleo-weathering crust from the Vihterpalu drill core has evolved on magnetite-rich amphibolite parent rock. It is characterised by a considerably thin zone of pervasively weathered rock but exhibits complex compositional variations and clear mineral zonation.

The total thickness of the paleo-weathering crust is close to 34 metres. The transition from parent rock to weathering crust is gradational, and the lower boundary of the weathering crust could not be definitely determined in the core section. Isochemical weathering processes prevailed in the saprock part of the weathering profile.

The paleosol horizon had gone through intense weathering, with CIA and CIW index values reaching > 90. The zone exhibits a porous residual complex enriched in ferruginous phases and kaolinite.

Thin clay-rich saprolite has evolved on the part of the weathering profile affected by percolating meteoric water. In this zone, all significant primary minerals have been replaced by secondary ones showing distinctive clay mineral assemblage celadonite (glauconite)-illite-smectite-chlorite-kaolinite. The study is the first to report on a finding of celadonite (glauconite) in the paleo-weathering crust of the Estonian crystalline basement. The loss of alkali and alkaline earth metals and Fe oxidisation during weathering of saprolite were accompanied by the precipitation of secondary phyllosilicates and iron oxyhydroxides.

The mechanically weak part of the paleo-weathering profile in the Vihterpalu drill core extends about 20 m below the crystalline basement's upper surface. The most significant change in compressive strength properties of paleo-weathering crust occurs in the lower part of the weathering profile. The decrease of mechanical strength of the rock is likely related to the breakage of a primary mineral along intramineral micro-fissures and cleavage planes and the formation of secondary clay minerals along grain boundaries of the primary minerals. In the upper section of the paleo-weathering profile, rock stability decreases with the increase of secondary clay-minerals.

Acknowledgements

I wish to express my deepest gratitude to my supervisor, Rutt Hints, for her guidance, patience, and valuable insight throughout the making of this thesis. Without her persistent help this thesis would not have been executed.

I would also like to thank Toivo Kallaste and Siim Pajusaar for their help with my XRD and XRF analysis, Siim Nirgi from the Geological Survey of Estonia, for his help in attaining the drill core material, and Kristjan Urtson for his insight in microscopy and thin section making.

Finally, I would like to pay my special regards to Karin Käär for her encouragement and understanding.

References

Bogdanova, S., Gorbatschev, R., Skridlaite, G., Soesoo, A., Taran, L., & Kurlovich, D. (2015). Trans-Baltic Palaeoproterozoic correlations towards the reconstruction of supercontinent Columbia/Nuna. *Precambrian Research, 259*, 5–33.

Driesea, S., Medaris, J. L., Kirsimäe, K., Somelar, P., & Stinchcomb, G. (2018). Oxisolic processes and geochemical constraints on duration of weathering for Neoproterozoic Baltic paleosol. *Precambrian Research, 310*, 155–178.

Drits, V. A., Zviagina, B. B., McCarty, D. K., & Salyin, A. L. (2010). Factors responsible for crystal-chemical variations in the solid solutions from illite to aluminoceladonite and from glauconite to celadonite. *American Mineralogist, 95 (2-3)*, 348–361.

Fedo, C. M., Nesbitt, H. W., & Young, G. (1995). Unraveling the effects of potassium metasomatism in sedimentary rocks and paleosols, with implications for paleoweathering conditions and provenance. *Geology, 23 (10)*, 921–924.

Harland, W. B. (2007). Origins and assessment of snowball Earth hypotheses. *Geological Magazine, 144 (04)*, 633–642.

Harnois, L. (1988). The CIW index: a new chemical index of weathering. *Sedimentary Geology, 55 (3-4)*, 319–322.

Holland, H. D. (2006). The oxygenation of the atmosphere and oceans. *Philosophical Transactions of the Royal Society B: Biological Sciences, 361 (1470),* 903–915.

Kivisilla, J., Niin, M., & Koppelmaa, H. (1999). Catalogue of chemical analyses of major elements in the rocks of the crystalline basement of Estonia. *Unpublished report.* Geological Survey of Estonia, Tallinn.

Kuuspalu, T., Vanamb, V., & Utsal, K. (1971). About the mineralogy of the crust of weathering of the Estonian crystalline basement. *Tartu Riikliku Ülikooli Toimetised, 286,* 52–163.

Liivamägi, S., Somelar, P., Vircava, I., Mahaney, W.C., Kirs, J., Kirsimäe, K., (2015). Petrology, mineralogy and geochemical climofunctions of the Neoproterozoic Baltic paleosol. *Precambrian Research, 256,* 170–188

Liivamägi, S., Kirsimäe, K., Somelar, P., & Kirs, J. (2012). Precambrian palaeosol from Baltica – reconstructing the Neoproterozoic climate. *Goldschmidt 2012 Conference Abstracts*, 5–37.

Liivamägi, S., Kirsimäe, K., Somelar, P., Kirs, J., & & Vircava, I. (2014). Neoproterozoic Baltic paleosol – clay mineralogy and paleoclimatic interpretation. *Programme and Abstract Book*, 148–148.

Merdith, A. S., Collins, A. S., Williams, S. E., Pisarevsky, S., Foden, J. D., Archibald, D. B., Blades M. L., Alessico, B. L., Armistead, S., Plavsa, D., Clark, C. & Müller, R. D. (2017). A full-plate global reconstruction of the Neoproterozoic. *Gondwana Research, 50*, 84–134.

Meunier, A. (2005). *Clays*. *Springer-Verlag, Berlin-Heidelberg*, 472 pp.

Middelburg, J. J., Weijden, C. H., & Woittiez, J. R. (1988). Chemical processes affecting the mobility of major, minor and trace elements during weathering of granitic rocks. *Chemical Geology, 68 (3-4)*, 253–273.

Munsell Colour (2012). *Munsell Soil Color Book*.

Nesbitt, H. W., & Young, G. M. (1982). Early Proterozoic climates and plate moyions inferred from major element chemistry of lutites. *Nature, 299*, 715–717.

Niin, M. (2002). Non-acid igneous rocks of the crystalline basement of Estonia. *Bulletin of the Geological Survey of Estonia, 10,* 4–19.

Parker, A. (1970). An index of weathering for silicate rocks. *Geological Magazine, 107 (6)*, 501–504.

Pierrehumbert, R., Abbot, D., Voigt, A., & Koll, D. (2011). Climate of the Neoproterozoic. *Annual Review of Earth and Planetary Sciences, 39*, 417–460.

Puura, V., Klein, V., Koppelmaa, H., & Niin, M. (1997). Precambrian basement. *In: Raukas, A., Teedumäe, A. (ed.), Geology and Mineral Resources of Estonia.* Estonian Academy Publishers, Tallinn. 27–34.

Puura, V., Vaher, R., Klein, V., Koppelmaa, H., Niin, M., Vanamb, V., & Kirs, J. (1983). The Crystalline Basement of Estonian Territory. *Russian Academy of Sciences.* Nauka, Moskva. 208 pp.

Rothman, D. H., Hayes, J. M., & Summons, a. R. (2003). Dynamics of the Neoproterozoic carbon cycle. *PNAS, 100 (14)*, 8124–8129.

Rämö, O., Huhma, H., & Kirs, J. (1996). Radiogenic isotopes of the Estonian and Latvian rapakivi granite suites: new data from the concealed Precambrian of the East European Craton. *Precambrian Research, 79 (3-4)*, 209–226.

Scott, K., & Pain, P. (2009). *Regolith Science.* Springer, Netherlands. 462 pp.

Sitdikova, L., Victor, I., Sidorova, E., & Khristoforova, D. A. (2015). Petrological geodynamic model for the evolution of the crystalline basement of the eastern russian plate. *Procedia Earth and Planetary Science, 15*, 585–589.

Soesoo, A., Nirgi, S., & Plado, J. (2020). The evolution of the Estonian Precambrian basement: geological, geophysical and geochronological constraints. *Proceedings of the Karelian Research Centre of the Russian Academy of Sciences, 2*, 1–25.

Soesoo, A., Puura, V., Kirs, J., Petersell, V., Niin, M., & All, T. (2004). Outlines of the Precambrian basement of Estonia. *Proceedings of the Estonian Academy of Sciences. Geology*, 149–164.

Townsend, F. (1985). Geotechnical characteristics of residual soils. *Journal of Geotechnical Engineering, 111 (1)*, 77–92.

Vanamb, V., & Kirs, J. (1990). Clay minerals from aluminous gneiss weathering crust of the Estonian crystalline basement. *Tartu Riikliku Ülikooli Toimetised, 885*, 23–37.

Vanamb, V., & Puura, V. (1983). Short report of the crust of weathering of the crystalline rocks. *In: Viiding, H. (ed.), The Crystalline Basement of Estonian Territory.* Nauka, Moskva. 173–180.

Vanamb, V., Kuuspalu, T., & Utsal, K. (1980). On the mineralogical zoning of the crust of weathering of the Estonian crystalline basement. *Tartu Riikliku Ülikooli Toimetised, 527*, 149–166.

Wilson, M. J. (2004). Weathering of the primary rock-forming minerals: processes, products and rates. *Clay Minerals, 39 (3)*, 233–266.

Appendix

Depth interval (m)	LOI 950°C	SiO_2 (%)	TiO_2 (%)	Al_2O_3 (%)	Fe_2O_3 (%)	MnO (%)	MgO (%)	CaO (%)	Na_2O (%)	K_2O (%)
204.10-204.15	9.53	31.93	2.19	25.01	29.53	0.05	0.57	0.20	0.05	0.38
204.20-204.24	8.54	28.19	2.89	22.19	37.07	0.12	0.47	0.21	0.06	0.18
205.40-205.50	5.31	41.85	2.30	15.27	26.25	0.05	2.72	0.60	0.07	5.28
205.90-206.00	8.00	41.26	1.95	16.29	19.47	0.13	4.29	2.67	0.04	5.88
206.15-206.20	13.10	26.43	1.53	10.95	30.08	0.32	8.35	5.91	0.02	3.32
206.92-207.00	8.41	38.61	1.95	15.33	22.38	0.16	4.09	3.14	0.06	5.70
207.85-207.80	7.76	39.58	1.73	14.82	22.90	0.15	4.74	2.46	0.04	5.52
208.30-208.40	9.49	36.50	1.95	12.07	24.91	0.19	6.12	3.88	0.06	4.87
208.96-209.00	11.53	32.69	1.80	9.69	28.08	0.26	6.47	5.34	0.04	4.14
209.70-209.80	3.95	39.03	1.96	12.89	24.19	0.19	8.73	6.98	0.68	1.25
211.20-211.24	2.78	38.85	1.65	15.34	20.70	0.17	7.83	11.61	0.72	0.41
212.25-212.30	7.55	38.75	1.54	12.17	23.37	0.15	8.58	5.06	0.32	2.71
214.60-214.70	1.95	38.80	1.83	14.87	21.40	0.14	8.51	11.56	0.78	0.29
216.30-216.40	4.69	42.67	1.68	11.71	22.23	0.19	9.89	4.57	0.43	2.04
218.75-218.85	2.42	39.76	1.73	14.58	20.54	0.15	9.74	9.65	0.76	0.49
220.65-220.72	3.05	35.98	2.26	11.73	28.87	0.17	9.19	7.36	0.61	1.19
221.55-221.67	6.94	40.25	1.55	14.13	19.22	0.09	11.78	1.62	0.58	4.05
223.80-223.88	1.16	39.48	1.86	11.45	22.35	0.19	10.48	12.27	0.65	0.15
224.60-224.67	1.80	40.89	1.46	15.15	18.05	0.16	8.62	12.65	0.75	0.27
227.15-227.26	2.08	37.63	1.92	13.56	23.50	0.17	9.87	10.68	0.60	0.21
229.05-229.10	0.92	39.91	1.57	15.74	18.07	0.15	7.73	14.92	0.74	0.06
233.10-233.25	2.31	39.00	1.63	13.98	20.94	0.18	9.41	11.49	0.76	0.33
237.10-237.18	1.10	42.11	1.12	16.44	15.26	0.17	8.09	14.44	0.88	0.19

Appendix 1. Chemical composition of bulk samples from the paleo-weathering crust, Vihterpalu F332 drill core.

Depth	Quartz	Calcite	Dolomite	Orthoclase	Mg-hornblend	Kaolinite	Chlorite	Anatase	Hematite	Magnetite	Celadonite	Ilmenite	Anorthite	Augite	Clay (I-S, S, Cor)
204.10-204.15	0.6					43.3		2.5	23.4						30.2
204.20-204.24	0.2					36.3		1.8	33.1						28.6
205.40-205.50	2.6			10.7		6.0	1.9	1.2	15.8						61.7
205.90-206.00	0.2		8.1	17.7		5.2	8.1	1.9	8.7	1.3	12.3				36.5

206.15-206.20	0.7		22.4	12.2		5.6	6.3	0.6	14.5						37.8
206.92-207.00	0.2		8.8	14.5		5.6	1.6	0.9	6.6	4.2	15.2	1.1			41.2
207.85-207.80	1.2		7.8	15.7		6.0	5.4	0.8	7.1	3.3	14.1	0.7			37.8
208.30-208.40	2.7		13.3	9.9		7.2	7.3	1.1	9.1	2.9	17.2	0.1			29.2
208.96-209.00	2.5		18.7	3.8		3.8	1.6	0.7	11.7	2.5	17.0	0.5			37.0
209.70-209.80	0.6	0.6		4.0	36.9	4.6	2.1	0.1	6.5	6.0		1.0	2.3		35.3
211.20-211.24	0.2	0.7	0.7	0.7	28.7	1.3	0.4		3.8	5.6		1.1	23.5	3.3	30.0
212.25-212.30	0.4	0.4	0.9	7.1	10.7	5.9	0.6	0.3	7.6	2.0		0.8	1.9		61.4
214.60-214.70	0.2	0.1	0.7		25.9	1.2	0.3		6.6	3.8		1.5	21.3	11.3	27.2
216.30-216.40	1.1	0.1		4.0	26.0	3.1	2.1	0.3	9.7	1.4		1.3	0.6		32.0
218.75-218.85	0.1	0.1		0.9	37.2	1.7	0.3		4.1	6.2		0.8	16.6	0.1	37.0
220.65-220.72	0.1		0.7	3.0	36.3	3.7	3.4	0.1	7.0	6.8		0.2	0.7	0.8	53.2
221.55-221.67	1.3	0.8	0.6	9.2	2.5	8.8	1.4	0.5	6.8	0.6	14.3				31.1
223.80-223.88	0.2		1.6		19.1	0.2	0.4		2.8	6.1		1.5	17.2	19.7	27.8
224.60-224.67	0.4	0.1	0.5		22.3	1.5	0.6		3.3	3.9		1.0	23.2	15.2	30.8
227.15-227.26	0.3	0.2	0.4		19.6	1.8	1.4		6.7	6.9		1.5	18.6	12.0	19.5
229.05-229.10	0.1	0.5	0.7		13.9	0.5	0.4			8.2		1.6	30.0	24.7	29.8
233.10-233.25	0.1	0.2	0.5		25.1	2.7	2.7		3.1	5.9		1.0	18.0	11.0	20.8
237.10-237.18	0.0	0.7	1.5		38.3		1.8		0.3	4.9		0.7	24.6	6.4	100.0

Appendix 2. Semiquantitative mineral composition of the paleo-weathering crust, Vihterpalu F332 drill core.

Lisa
rektori 07.04.2020 käskkirjale nr 1-8/17

Lihtlitsents lõputöö reprodutseerimiseks ja lõputöö üldsusele kättesaadavaks tegemiseks[1]

Mina, Carina Potagin

1. Annan Tallinna Tehnikaülikoolile tasuta loa (lihtlitsentsi) enda loodud teose Composition and geotechnical properties of paleo-weathering crust from the Vihterpalu F332 drill core

mille juhendaja on Rutt Hints,

1.1 reprodutseerimiseks lõputöö säilitamise ja elektroonse avaldamise eesmärgil, sh Tallinna Tehnikaülikooli raamatukogu digikogusse lisamise eesmärgil kuni autoriõiguse kehtivuse tähtaja lõppemiseni;

1.2 üldsusele kättesaadavaks tegemiseks Tallinna Tehnikaülikooli veebikeskkonna kaudu, sealhulgas Tallinna Tehnikaülikooli raamatukogu digikogu kaudu kuni autoriõiguse kehtivuse tähtaja lõppemiseni.

2. Olen teadlik, et käesoleva lihtlitsentsi punktis 1 nimetatud õigused jäävad alles ka autorile.

3. Kinnitan, et lihtlitsentsi andmisega ei rikuta teiste isikute intellektuaalomandi ega isikuandmete kaitse seadusest ning muudest õigusaktidest tulenevaid õigusi.

_______________ (kuupäev)

[1] *Lihtlitsents ei kehti juurdepääsupiirangu kehtivuse ajal vastavalt üliõpilase taotlusele lõputööle juurdepääsupiirangu kehtestamiseks, mis on allkirjastatud teaduskonna dekaani poolt, välja arvatud ülikooli õigus lõputööd reprodutseerida üksnes säilitamise eesmärgil. Kui lõputöö on loonud kaks või enam isikut oma ühise loomingulise tegevusega ning lõputöö kaas- või ühisautor(id) ei ole andnud lõputööd kaitsvale üliõpilasele kindlaksmääratud tähtajaks nõusolekut lõputöö reprodutseerimiseks ja avalikustamiseks vastavalt lihtlitsentsi punktidele 1.1. jq 1.2, siis lihtlitsents nimetatud tähtaja jooksul ei kehti.*